

# A two year comparison between HF radar and ADCP current measurements in Liverpool Bay

*AM Robinson and LR Wyatt, Department of Applied Mathematics, University of Sheffield  
Mj Howarth, National Oceanography Centre*

---

This study compares current measurements between HF WERA radar and Acoustic Doppler Current Profilers (ADCPs) in Liverpool Bay using a two-year time series from 2006 to 2008. Radar measurements are shown to agree well with those of ADCPs, having directional differences of less than  $3^\circ$ , amplitude correlations greater than 0.93, and small root mean square differences. Using Least Squares Harmonic Analysis for tidal decomposition radar measurements are shown to best capture surface effects. The effects of the North Hoyle wind farm on current measurement accuracy are found to be negligible, while effects from cross-over angle in the region of the wind farm are of greater importance.

---

---

## LEAD AUTHOR'S BIOGRAPHY

After completing a bachelors degree in Environmental Physics at Lancaster University, Alice Robinson took a break from education and worked with the (UK) Environment Agency before starting her PhD studies at The University of Sheffield in 2006. The main focus of her thesis is the interaction between ocean sensing HF radar and wind turbines.

---

## INTRODUCTION

**L**iverpool Bay is a shallow shelf sea that experiences many coastal processes with influencing factors both natural and human. A range of dynamic processes including freshwater inputs, strong tidal influences, large tidal ranges ( $>10\text{m}$ ) and shallow water depths ( $<50\text{m}$ ) are all present, as well as a densely populated coast with industrial and recreational activities.<sup>1,2</sup> Freshwater inputs from the Dee, Ribble and Mersey rivers can discharge up to  $600\text{m}^3\text{s}^{-1}$  each<sup>3</sup> causing complicated horizontal and vertical gradients. Tidal forcing in Liverpool Bay is the dominant current process, in particular the semidiurnal  $M_2$  tide with maximum spring amplitudes up to  $1\text{ms}^{-1}$ .<sup>4</sup> Waves are only locally generated in the Irish Sea so there is an absence of any long period swell, and significant wave heights do not exceed  $5.5\text{m}$ .<sup>2</sup>

The Liverpool Bay Coastal Observatory (for key features see Fig 1) was established by the National Oceanography Centre (NOC) in 2002. It operates and maintains a variety of equipment including a SmartBuoy, High Frequency (HF) radar, X-band radar, two Acoustic Doppler Current Profilers (ADCPs), tide gauges and satellite imagery as well as conducting regular ferry measurements.<sup>2</sup> Various parameters are measured including currents, winds, significant wave heights, wave periods, salinity, temperature and suspended sediment.<sup>1</sup>

Continuous measurement is important as long time series datasets ensure measurement techniques sample large varieties of anthropogenic influences and environmental conditions as well as identifying trends, dynamics, and their changes. Models of these processes undergo constant testing and development, also requiring the continual collection and assessment of data; for example the Proudman Oceanographic Laboratory Coastal Ocean Modelling System (POLCOMS) uses data to improve the value of its results testing model outputs against events as they happen.<sup>5</sup> Data can also be assimilated into models to keep them on track and to validate and improve their underpinning physical principles.

HF radar current measurements in Liverpool Bay have been assessed by comparison with ADCP using a two-year time series from January 2006 to December 2007, a much longer period than previously compared. The ADCP and HF

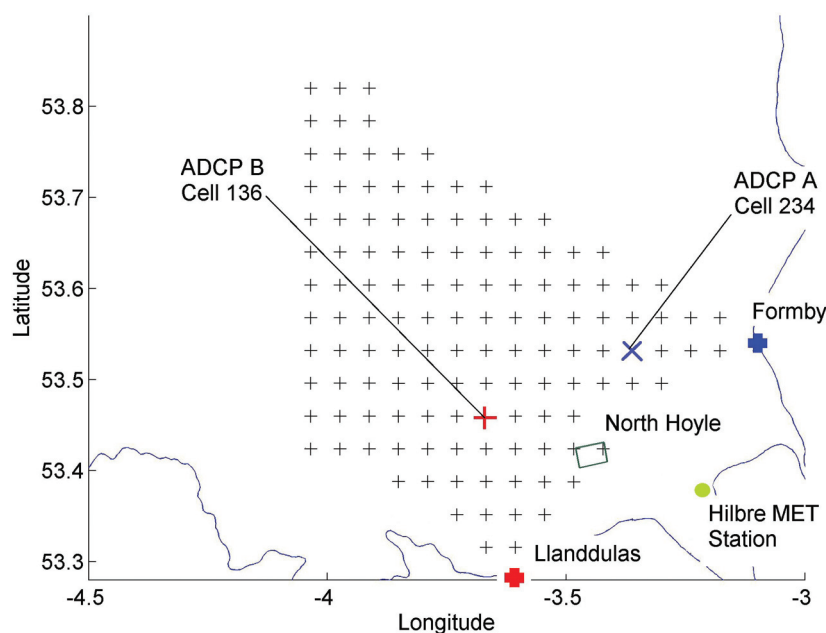


Fig 1: Liverpool Bay features. Hilbre Island MET station, ADCPs at sites A and B, indicated with a bold blue 'x' and bold red '+' respectively, HF radar operational sites Llanddulas and Formby, dual current and wave coverage cells, the centre of which shown by a small '+', and the North Hoyle wind-farm

radar have both been established current measurement techniques for several years and operate on the principle of determining measurements from frequency shifts of a known signal. HF radar utilises Bragg scattering characteristics of the backscatter from ocean waves with half the radar transmitting wavelength, first identified by Crombie.<sup>6</sup> The associated frequency shift in the first-order backscatter signal determines surface currents while the relative amplitude difference from currents moving directly away and towards the radar are used for wind directions. The second-order backscatter measures wave parameters, the theoretical formulation for which was set out in the 1970s.<sup>7, 8</sup> Vigorous testing of HF radar wave measurement techniques has recently included the European Radar Ocean Sensing project (EuroROSE)<sup>9</sup> and testing of the Pisces HF radar.<sup>10</sup> The ADCPs operate by emitting mono-frequency sonar pulses in known directions from a transducer into the water column. The pulse is then scattered off any suspended particles causing a Doppler frequency shift from which the component velocity along the direction of each beam averaged over a range cell is calculated.<sup>11</sup>

There have been several studies on the current measurement agreement between HF radars and ADCPs as well as other fixed moorings such as current meters and buoys.<sup>2, 12, 13, 14, 15, 16</sup> These have provided better understanding of the physical processes involved, allowed ongoing performance assessment and motivated improvements in measurement capabilities. They involve the comparison of radar surface current measurements with near surface current (exact depth depending on the particular instruments and deployment) obtained from the *in-situ* measurement device. Table 1 summarises several studies between HF radar and fixed moorings, in particular ADCPs, and is intended for reference purposes but is by no means complete. These studies share similar characteristics with Liverpool Bay and/or the HF WERA radar utilised by NOC, as well as comparing a mixture of current radials, dual east (u) and west (v) current components, and dual current vectors. Types of radar and fixed mooring vary and include the Ocean Surface Current Radar (OSCR),<sup>12,13</sup> the Coastal Ocean

Dynamics Applications Radars (CODAR),<sup>12,15,16</sup> and the WERA RAdar (WERA radar).<sup>2</sup> In spite of all these studies there remains some scepticism about the accuracy of HF radar current measurements and it is hoped this two-year comparison will provide further solid evidence to confirm the place of HF radar as an operational current measurement technology.

Spatial and temporal averaging of currents measured by the ADCP and HF radar is inherent in their methodology and improves the accuracy of each technique but, by nature, impacts on their current measurement comparison. Spatial averaging of the radar occurs horizontally in range and azimuth according to the radar configuration and from the surface to a depth of  $\lambda/8\pi$ , where  $\lambda$  is the transmitted wavelength.<sup>17</sup> The bed mounted ADCP current measurement is averaged through 1m vertical bins the top of which will always be approximately 2m below the surface. Physical mechanisms such as the Ekman-veering<sup>18</sup> and Stokes drift will cause differences and during strong wind-forced conditions are considered to be the dominating difference sources.<sup>19</sup> A geometric model applied by Chapman and Graber<sup>19</sup> concluded an upper bound for the root mean square (rms) difference of the radar derived dual current vector to be  $15\text{cm/s}^{-1}$  and predicted a lower rms difference for radar derived currents of  $7\text{--}8\text{cm/s}^{-1}$ . This was for the case when no error associated with the cross-over angle, the angle between the look directions of two radar beams for a particular dual current measurement, was present.<sup>4</sup>

Clutter is another error source. This will generally be independent to each measurement technique – for example radio frequency interference (RFI) affects radar but not the ADCP. Physical objects such as ships, buoys, land and wind turbines are more likely to affect the radar as its spatial coverage is so much greater and the ocean surface clutter is directly observed. A clutter source specific to the Liverpool Bay HF radar is wind farms. There are currently three operational wind farms – Rhyl Flats (RWF), North Hoyle (NHWF) and Burbo Bank (BBWF) – with 25 to 30 turbines. Gwent-y-Mor wind farm is also proposed for the region. This will become ever more problematic as wind farms and wind turbines increase in size and number as there is an obvious influence on scattering

characteristics and noise levels in their vicinity.<sup>2</sup> Established in 2003 NHWF is the oldest wind farm in Liverpool Bay. This region of radar footprint is investigated for any degradation of the radar current measurement and as a start to fully understanding the radar-wind farm interaction. Howarth<sup>2</sup> also briefly considered this region and concluded there was no obvious impact on the current measurements.

The error sources and the comparison of HF radar wave measurements<sup>20, 21</sup> are not discussed any further here.

## ADCP

NOC operate two 600kHz ADCPs at sites A and B shown in Fig 1. These are bed-mounted emitting four orthogonal beams inclined 20° from the vertical. Backscatter is returned to the transducers from particles in the water column. This allows current velocity in the direction of the transducer to be calculated from any Doppler shift with range-gating being used to determine the position of the scattering particles. Data is based on ensembles of 100 pings every 10 minutes and recorded in 1m bins from 2.5m above the bed through the height of the water column to 2m below the surface, a limiting depth due to increasingly prevalent side-lobes.

ADCPs used by NOC are generally considered to have an accuracy of 0.2% of the measured current magnitude  $\pm 0.5\text{cm/s}^{-1}$ .<sup>22</sup> The ADCP accuracy is, however, highly variable and dependent on several factors including the installation characteristics where for non-zero pitch and roll angles individual beam velocities are at different vertical depths in the water column. For example a roll of just 1° and a current magnitude of  $50\text{cm/s}^{-1}$  typically introduce errors of  $1\text{cm/s}^{-1}$ .<sup>23</sup> Data is available in near to real time via satellite. Regular servicing is carried out every 4–6 weeks<sup>1</sup> during the summer and becomes less frequent during winter months. Inconsistencies can arise in longer ADCP current time series as different instruments of the same type have been deployed at locations A and B and, due to the logistics of maintenance and repair, gaps in the time series can be large.

## HF RADAR

HF radar is a widely used remote ocean sensing tool for measuring currents, winds and waves via ground-wave propagation. Crombie<sup>6</sup> first identified the relationship between the transmitted wavelength and resonant backscatter from the ocean surface from waves of half the transmitted wavelength, referred to as Bragg scattering. This enabled the measurement of radial current speeds in the direction of the radar look angle via a frequency shift in the Doppler spectrum of the backscattered signal.

Several HF radar systems have emerged over the years, the first of which was CODAR,<sup>8</sup> developed by the National Oceanic and Atmospheric Administration (NOAA). CODAR was designed for compact rapid deployment and uses direction finding techniques to map ocean currents. Barrick<sup>7</sup> mathematically related the second order Doppler spectra to the ocean wave spectrum and HF radars were developed to provide measurements of the sea state. These included the

phased array Pisces radar developed in the UK in the late eighties<sup>24</sup> and the WERA, developed by the University of Hamburg<sup>25, 26</sup> which can be arranged for direction finding or phased array measurements.

The Liverpool Bay Coastal Observatory has operated a HF WERA radar since 2005. It consists of two sites each with a co-located transmit and receive antenna measuring radial currents (currents travelling directly towards or away from the radar) which are then resolved for the dual current vectors as well as wind and wave parameters. Operating at 30W and approximately 13MHz (the exact operating frequencies differ to allow simultaneous data acquisition) each radar transmits a frequency modulated continuous wave (FMCW). The receive antenna is a 16 linear phased array whip antenna parallel to the coast and with  $\lambda/2$  spacing, where  $\lambda$  is the transmit wavelength, and uses beamforming<sup>27</sup> to determine bearing angle.

Optimum angular resolution for the WERA system is given by  $\lambda/D$ , where  $\lambda$  is the transmit wavelength and  $D$  is the receive antenna array length.<sup>27</sup> In Liverpool Bay this is 7.6°. Emery<sup>16</sup> calculated the bearing accuracy of the CODAR radar to be in the region of 4–10° and any angular agreement between the radar and ADCP of this order is acceptable. At 13MHz the current is depth averaged to approximately 1m,<sup>17</sup> temporally averaged over 8 min, 52 sec every 20 min and recorded on a 4km rectangular grid up to a 75km range. Fig 1 shows the region of dual current and wave coverage.

Data from the radar is available in near to real time with excellent spatial coverage of near surface currents compared to those of fixed moorings, such as buoys, drifters and ADCPs. The radar configuration and *in-situ* conditions are fairly constant and yield a more consistent time series with fewer and smaller gaps than that of the ADCPs.

## HF RADAR/ADCP COMPARISONS

The results compared in this study, shown in Table 1, range over the past 15 years. Accuracy and improvements during this period are mainly due to analysis and processing techniques as the physical measurement techniques for current measurement have been established for many years prior to this. Most advances in HF over the past 15 years have been in the development of wave parameter estimations.<sup>5,9,10,26</sup>

Physical system set-up is incredibly important. Radar measurement range and the extent of the radar footprint are determined by a combination of factors yet can be limited due to physical set-up in the radar siting and orientation. The deployment environment is also dynamic and for longer time series maintaining a consistency is important; however, it is only with the longer time series that a particular radar site will have the opportunity to be developed and measurements optimised.

HF radars and ADCP radial current correlations in previous studies vary from as low as 0.58<sup>12</sup> to 0.88.<sup>16</sup> Radial-ADCP current comparisons are highly dependent on the physical situation of the radar and current orientation in relation to the radar measurement. Paduan<sup>28</sup> found increased correlations when a high percentage of current was in the direction of the radar radial measurement, as was the case for the Santa Cruz (SC) and Point Pinos (PP), compared to when

Reference	Radar	Location	Frequency	Mooring type	Measurement details	r	RMSD cms <sup>-1</sup>	Mean current speeds cms <sup>-1</sup> (direction deg)
Fernandez and Paduan (1996) Monterey Bay	OSCR	S.C. M.L.	25.4 MHz	ADCP (bin centered at 9m depth)	Radial Currents	0.72 0.58	5.7 6.4	
	CODAR	S.C. PP	12.2 MHz 113.7 MHz		u v	0.4 0.66	8.5 9.5	
Paduan and Rosenfeld (1996) Monterey Bay	CODAR	S.C. PP M.L.	12.5 MHz 12.5 MHz 25.4 MHz	ADCP (bin centered at 9m depth)	Vector Currents (3 radial current derived)	u 0.58 v 0.83	6.2 10.8	20 (E) 30 (E) 20 (E) 30 (E)
				Ship mounted ADCP (bin centered at 12m depth)		u -0.25 v 0.45	13.2 8.4	
Graber et al. (1997) Cape Hatteras North Carolina	OSCR	C.H.  Station B1 Station B2 Station DE	25.4 MHz	OSCR vector currents			<b>speed</b>	BI 18.6 ± 10.7 B2 39.8 ± 23.5 DE 34.9 ± 18.8
							<b>θ (deg)</b>	
							20.5 18.2 20.1	41 46 51
							8.1 13.3 6.9 6.3	≈25 (E)  ≈25 (E)
Teague et al. (2001) Chesapeake Bay	MFCR	C.B.	4.8 MHz 13.4 MHz	ADCP	u v u v	0.87  0.92		
Kelly et al. (2003) West Florida Shelf	CODAR	W.F.S.	25 MHz	ADCP	Along-shelf Cross-shelf	0.92 0.62	- -	ADCP Radar -7 ± 12 -2 ± 5 -9.8 ± 17 -0.8 ± 5
					Dual Radar, complex current magnitude (phase - degrees)	0.87 (-5.7)	-	
Emery et al. (2004) Santa Maria Basin	CODAR	RFG COP	13 MHz	ADCP	Radial Currents	0.50 0.60	12 11	20 (E) 20 (E)

Table 1 Continued										
Reference	Radar	Location	Frequency	Mooring type	Measurement details	r	RMSD cms <sup>-1</sup>	Mean current speeds cms <sup>-1</sup> (direction deg)		
Kaplan <i>et al.</i> (2005) <sup>35</sup> Bogega Bay	CODAR	B.M.L. P.R.	12.5 MHz <sub>z</sub>	4 x ADCP - Buoy mounted, down- ward looking (bin height of 5 or 6m depth)	Dual Radar; complex current magnitude (phase – degrees)	0.90 (–3.1)	13.0	20 (E)		
						0.86 (–4.2)	14.1			
						0.89 (0.79)	15.2			
						0.78 (29.1)	19.1			
						0.89	10.1			
						0.86	12.1			
						0.91	11.7			
						0.87	11.4			
						0.92	8.2			
						0.85	7.3			
0.83	9.6									
0.04	15.4	20 (E)								
Paduan <i>et al.</i> (2006) Monterey Bay	SeaSonde CODAR		S.C. N.P.S. P.P. M.L.	13 MHz <sub>z</sub> 13 MHz <sub>z</sub> 13 MHz <sub>z</sub> 25 MHz <sub>z</sub>	ADCP/Drifters (Downward looking ADCP Measurements 12–20m below surface)	Radial Currents	0.62//0.74	18.1//12.7	25 (E)	
							0.57//0.79	17.6//10.4		
							0.62//0.77	16.6//10.4		
							0.34//0.72	12.4//10		
							0.85	16.2		30(E) 35(E) 20 (E) Zonal - 50 (E)
							0.87	15.6		
							0.34	24.6		
							0.84	17.5		
							0.71	19.6		
		Radial Currents					Meridional	26.6		
25.2										
36.6										
22.4										
0.73	25.0	Zonal - 50 (E)								
Shipboard ADCP 5–10m below surface	Radial Currents		0.77	Meridional - 30 (E)						
			0.85							
			0.38							
		0.79								
0.73	25.0	Zonal - 50 (E)								
Drifter Buoy	Radial Currents		0.77	Meridional - 30 (E)						
			0.85							
			0.38							
		0.79								
0.73	25.0	Zonal - 50 (E)								
Shipboard ADCP 5–10m below surface	Radial Currents		0.77	Meridional - 30 (E)						
			0.85							
			0.38							
		0.79								
0.73	25.0	Zonal - 50 (E)								
Drifter Buoy	Radial Currents		0.77	Meridional - 30 (E)						
			0.85							
			0.38							
		0.79								
0.73	25.0	Zonal - 50 (E)								
Shipboard ADCP 5–10m below surface	Radial Currents		0.77	Meridional - 30 (E)						
			0.85							
			0.38							
		0.79								
0.73	25.0	Zonal - 50 (E)								
Drifter Buoy	Radial Currents		0.77	Meridional - 30 (E)						
			0.85							
			0.38							
		0.79								
0.73	25.0	Zonal - 50 (E)								
Shipboard ADCP 5–10m below surface	Radial Currents		0.77	Meridional - 30 (E)						
			0.85							
			0.38							
		0.79								
0.73	25.0	Zonal - 50 (E)								
Drifter Buoy	Radial Currents		0.77	Meridional - 30 (E)						
			0.85							
			0.38							
		0.79								
0.73	25.0	Zonal - 50 (E)								
Shipboard ADCP 5–10m below surface	Radial Currents		0.77	Meridional - 30 (E)						
			0.85							
			0.38							
		0.79								
0.73	25.0	Zonal - 50 (E)								
Drifter Buoy	Radial Currents		0.77	Meridional - 30 (E)						
			0.85							
			0.38							
		0.79								
0.73	25.0	Zonal - 50 (E)								
Shipboard ADCP 5–10m below surface	Radial Currents		0.77	Meridional - 30 (E)						
			0.85							
			0.38							
		0.79								
0.73	25.0	Zonal - 50 (E)								
Drifter Buoy	Radial Currents		0.77	Meridional - 30 (E)						
			0.85							
			0.38							
		0.79								
0.73	25.0	Zonal - 50 (E)								
Shipboard ADCP 5–10m below surface	Radial Currents		0.77	Meridional - 30 (E)						
			0.85							
			0.38							
		0.79								
0.73	25.0	Zonal - 50 (E)								
Drifter Buoy	Radial Currents		0.77	Meridional - 30 (E)						
			0.85							
			0.38							
		0.79								
0.73	25.0	Zonal - 50 (E)								
Shipboard ADCP 5–10m below surface	Radial Currents		0.77	Meridional - 30 (E)						
			0.85							
			0.38							
		0.79								
0.73	25.0	Zonal - 50 (E)								
Drifter Buoy	Radial Currents		0.77	Meridional - 30 (E)						
			0.85							
			0.38							
		0.79								
0.73	25.0	Zonal - 50 (E)								
Shipboard ADCP 5–10m below surface	Radial Currents		0.77	Meridional - 30 (E)						
			0.85							
			0.38							
		0.79								
0.73	25.0	Zonal - 50 (E)								
Drifter Buoy	Radial Currents		0.77	Meridional - 30 (E)						
			0.85							
			0.38							
		0.79								
0.73	25.0	Zonal - 50 (E)								
Shipboard ADCP 5–10m below surface	Radial Currents		0.77	Meridional - 30 (E)						
			0.85							
			0.38							
		0.79								
0.73	25.0	Zonal - 50 (E)								
Drifter Buoy	Radial Currents		0.77	Meridional - 30 (E)						
			0.85							
			0.38							
		0.79								
0.73	25.0	Zonal - 50 (E)								
Shipboard ADCP 5–10m below surface	Radial Currents		0.77	Meridional - 30 (E)						
			0.85							
			0.38							
		0.79								
0.73	25.0	Zonal - 50 (E)								
Drifter Buoy	Radial Currents		0.77	Meridional - 30 (E)						
			0.85							
			0.38							
		0.79								
0.73	25.0	Zonal - 50 (E)								
Shipboard ADCP 5–10m below surface	Radial Currents		0.77	Meridional - 30 (E)						
			0.85							
			0.38							
		0.79								
0.73	25.0	Zonal - 50 (E)								
Drifter Buoy	Radial Currents		0.77	Meridional - 30 (E)						
			0.85							
			0.38							
		0.79								
0.73	25.0	Zonal - 50 (E)								
Shipboard ADCP 5–10m below surface	Radial Currents		0.77	Meridional - 30 (E)						
			0.85							
			0.38							
		0.79								
0.73	25.0	Zonal - 50 (E)								
Drifter Buoy	Radial Currents		0.77	Meridional - 30 (E)						
			0.85							
			0.38							
		0.79								
0.73	25.0	Zonal - 50 (E)								
Shipboard ADCP 5–10m below surface	Radial Currents		0.77	Meridional - 30 (E)						
			0.85							
			0.38							
		0.79								
0.73	25.0	Zonal - 50 (E)								
Drifter Buoy	Radial Currents		0.77	Meridional - 30 (E)						
			0.85							
			0.38							
		0.79								
0.73	25.0	Zonal - 50 (E)								
Shipboard ADCP 5–10m below surface	Radial Currents		0.77	Meridional - 30 (E)						
			0.85							
			0.38							
		0.79								
0.73	25.0	Zonal - 50 (E)								
Drifter Buoy	Radial Currents		0.77	Meridional - 30 (E)						
			0.85							
			0.38							
		0.79								
0.73	25.0	Zonal - 50 (E)								
Shipboard ADCP 5–10m below surface	Radial Currents		0.77	Meridional - 30 (E)						
			0.85							
			0.38							
		0.79								
0.73	25.0	Zonal - 50 (E)								
Drifter Buoy	Radial Currents		0.77	Meridional - 30 (E)						
			0.85							
			0.38							
		0.79								
0.73	25.0	Zonal - 50 (E)								
Shipboard ADCP 5–10m below surface	Radial Currents		0.77	Meridional - 30 (E)						
			0.85							
			0.38							
		0.79								
0.73	25.0	Zonal - 50 (E)								
Drifter Buoy	Radial Currents		0.77	Meridional - 30 (E)						
			0.85							
			0.38							
		0.79								
0.73	25.0	Zonal - 50 (E)								
Shipboard ADCP 5–10m below surface	Radial Currents		0.77	Meridional - 30 (E)						
			0.85							
			0.38							
		0.79								
0.73	25.0	Zonal - 50 (E)								
Drifter Buoy	Radial Currents		0.77	Meridional - 30 (E)						
			0.85							
			0.38							
		0.79								
0.73	25.0	Zonal - 50 (E)								
Shipboard ADCP 5–10m below surface	Radial Currents		0.77	Meridional - 30 (E)						
			0.85							
			0.38							
		0.79								
0.73	25.0	Zonal - 50 (E)								
Drifter Buoy	Radial Currents		0.77	Meridional - 30 (E)						
			0.85							
			0.38							
		0.79								
0.73	25.0	Zonal - 50 (E)								
Shipboard ADCP 5–10m below surface	Radial Currents		0.77	Meridional - 30 (E)						
			0.85							
			0.38							
		0.79								
0.73	25.0	Zonal - 50 (E)								
Drifter Buoy	Radial Currents		0.77	Meridional - 30 (E)						
			0.85							
			0.38							
		0.79								
0.73	25.0	Zonal - 50 (E)								
Shipboard ADCP 5–10m below surface	Radial Currents		0.77	Meridional - 30 (E)						
			0.85							
			0.38							
		0.79								
0.73	25.0	Zonal - 50 (E)								
Drifter Buoy	Radial Currents		0.77	Meridional - 30 (E)						
			0.85							
			0.38							
		0.79								
0.73	25.0	Zonal - 50 (E)								
Shipboard ADCP 5–10m below surface	Radial Currents		0.77	Meridional - 30 (E)						
			0.85							
			0.38							
		0.79								
0.73	25.0	Zonal - 50 (E)								
Drifter Buoy	Radial Currents		0.77	Meridional - 30 (E)						
			0.85							
			0.38							
		0.79								
0.73	25.0	Zonal - 50 (E)								
Shipboard ADCP 5–10m below surface	Radial Currents		0.77	Meridional - 30 (E)						
			0.85							
			0.38							
		0.79								
0.73	25.0	Zonal - 50 (E)								
Drifter Buoy	Radial Currents		0.77	Meridional - 30 (E)						
			0.85							
			0.38							
		0.79								
0.73	25.0	Zonal - 50 (E)								
Shipboard ADCP 5–10m below surface	Radial Currents		0.77	Meridional - 30 (E)						
			0.85							
			0.38							
		0.79								
0.73	25.0	Zonal - 50 (E)								
Drifter Buoy	Radial Currents		0.77	Meridional - 30 (E)						
			0.85							
			0.38							
		0.79								
0.73	25.0	Zonal - 50 (E)								
Shipboard ADCP 5–10m below surface	Radial Currents		0.77	Meridional - 30 (E)						
			0.85							
			0.38							
		0.79								
0.73	25.0	Zonal - 50 (E)								
Drifter Buoy	Radial Currents		0.77	Meridional - 30 (E)						
			0.85							
			0.38							
		0.79								
0.73	25.0	Zonal - 50 (E)								
Shipboard ADCP 5–10m below surface	Radial Currents		0.77	Meridional - 30 (E)						
			0.85							
			0.38							
		0.79								
0.73	25.0	Zonal - 50 (E)								
Drifter Buoy	Radial Currents		0.77	Meridional - 30 (E)						
			0.85							
			0.38							
		0.79								
0.73	25.0	Zonal - 50 (E)								
Shipboard ADCP 5–10m below surface	Radial Currents		0.77	Meridional - 30 (E)						
			0.85							
			0.38							
		0.79								
0.73	25.0	Zonal - 50 (E)								
Drifter Buoy	Radial Currents		0.77	Meridional - 30 (E)						
			0.85							
			0.38							
		0.79								
0.73	25.0	Zonal - 50 (E)								
Shipboard ADCP 5–10m below surface	Radial Currents		0.77	Meridional - 30 (E)						
			0.85							
			0.38							
		0.79								
0.73	25.0	Zonal - 50 (E)								
Drifter Buoy	Radial Currents		0.77	Meridional - 30 (E)						
			0.85							
			0.38							
		0.79								
0.73	25.0	Zonal - 50 (E)								
Shipboard ADCP 5–10m below surface	Radial Currents		0.77	Meridional - 30 (E)						
			0.85							
			0.38							
		0.79								
0.73	25.0	Zonal - 50 (E)								
Drifter Buoy	Radial Currents		0.77	Meridional - 30 (E)						
			0.85							
			0.38							
		0.79								
0.73	25.0	Zonal - 50 (E)								
Shipboard ADCP 5–10m below surface	Radial Currents		0.77	Meridional - 30 (E)						
			0.85							
			0.38							
		0.79								
0.73	25.0	Zonal - 50 (E)								
Drifter Buoy	Radial Currents		0.77	Meridional - 30 (E)						
			0.85							
			0.38							
		0.79								
0.73	25.0	Zonal - 50 (E)								
Shipboard ADCP 5–10m below surface	Radial Currents		0.77	Meridional - 30 (E)						
			0.85							
			0.38							
		0.79								
0.73	25.0	Zonal - 50 (E)								
Drifter Buoy	Radial Currents		0.77	Meridional - 30 (E)						
			0.85							
			0.38							
		0.79								
0.73	25.0	Zonal - 50 (E)								
Shipboard ADCP 5–10m below surface	Radial Currents		0.77	Meridional - 30 (E)						
			0.85							
			0.38							
		0.79								
0.73	25.0	Zonal - 50 (E)								
Drifter Buoy	Radial Currents		0.77	Meridional - 30 (E)						
			0.85							
			0.38							
		0.79								
0.73	25.0	Zonal - 50 (E)								
Shipboard ADCP 5–10m below surface	Radial Currents		0.77	Meridional - 30 (E)						
			0.85							
			0.38							
		0.79								
0.73	25.0	Zonal - 50 (E)								
Drifter Buoy	Radial Currents		0.77	Meridional - 30 (E)						
			0.85							
			0.38							
		0.79								
0.73	25.0	Zonal - 50 (E)								
Shipboard ADCP 5–10m below surface	Radial Currents		0.77	Meridional - 30 (E)						
			0.85							
			0.38							
		0.79								
0.73	25.0	Zonal - 50 (E)								
Drifter Buoy	Radial Currents		0.77	Meridional - 30 (E)						
			0.85							
			0.38							
		0.79								
0.73	25.0	Zonal - 50 (E)								
Shipboard ADCP 5–10m below surface	Radial Currents		0.77	Meridional - 30 (E)						
			0.85							
			0.38							
		0.79								
0.73	25.0	Zonal - 50 (E)								
Drifter Buoy	Radial Currents		0.77	Meridional - 30 (E)						
			0.85							
			0.38							
		0.79								
0.73	25.0	Zonal - 50 (E)								
Shipboard ADCP 5–10m below surface	Radial Currents		0.77	Meridional - 30 (E)						
			0.85							
			0.38							
		0.79								
0.73	25.0	Zonal - 50 (E)								
Drifter Buoy	Radial Currents		0.77	Meridional - 30 (E)						
			0.85							
			0.38							
		0.79								
0.73	25.0	Zonal - 50 (E)								
Shipboard ADCP 5–10m below surface	Radial Currents		0.77	Meridional - 30 (E)						
			0.85							
			0.38							
		0.79								
0.73	25.0	Zonal - 50 (E)								
Drifter Buoy	Radial Currents		0.77	Meridional - 30 (E)						
			0.85							
			0.38							
		0.79								
0.73	25.0	Zonal - 50 (E)								
Shipboard ADCP 5–10m below surface	Radial Currents		0.77	Meridional - 30 (E)						
			0.85							
			0.38							
		0.79								
0.73	25.0	Zonal - 50 (E)								
Drifter Buoy	Radial Currents		0.77	Meridional - 30 (E)						
			0.85							
			0.38							
		0.79								
0.73	25.0	Zonal - 50 (E)								
Shipboard ADCP 5–10m below surface	Radial Currents		0.77	Meridional - 30 (E)						
			0.85							
			0.38							
		0.79								
0.73	25.0	Zonal - 50 (E)								
Drifter Buoy	Radial Currents		0.77	Meridional - 30 (E)						
			0.85							
			0.38							
		0.79								
0.73	25.0	Zonal - 50 (E)								
Shipboard ADCP 5–10m below surface	Radial Currents		0.77	Meridional - 30 (E)						
			0.85							
			0.38							
		0.79								
0.73	25.0	Zonal - 50 (E)								
Drifter Buoy	Radial Currents		0.77	Meridional - 30 (E)						
			0.85							
			0.38							
		0.79								
0.73	25.0	Zonal - 50 (E)								
Shipboard ADCP 5–10m below surface	Radial Currents		0.77	Meridional - 30 (E)						
			0.85							
			0.38							
		0.79								
0.73	25.0	Zonal - 50 (E)								
Drifter Buoy	Radial Currents		0.77	Meridional - 30 (E)						
			0.85							
			0.38							

Table 1: A brief selection of results from key studies for use as a quick comparison. r is the correlation coefficient between the radars and moored current meters or ADCP's and RMSD is the root mean square difference.  $\theta$  is in reference to direction and is given in degrees. Mean current speeds are given where possible, however some are estimated (E) from current plots and should be treated with caution. Locations are Santa Cruz, SC, Moss Landing, ML, Points Pinos, PP, Chesapeake Bay, CB, Cape Hatteras, CH, West Florida Shelf, WFS, Refugio Beach, RFG, Coal Oil Point, COP, Santa Maria Basin, SM, Naval Postgraduate School, NPS, Bogega Marine Lab, BML, Point Reyes, PR, Noshappu, NS, Soya, SY, Sarufutsu, SR, and Liverpool Bay, LB. Radars are Ocean Surface Current Radar, OSCR, Coastal Ocean Dynamics Applications Radar, CODAR, Multi-Frequency Coastal Radar and WELAN Radar, WERA



it was not, as was the case for Moss Landing (ML) (see Table 1). The radial-ADCP comparison for this study is therefore expected to give mixed results with those from Formby, mainly orientated with the dominant east-west current, having better correlations than the Llanddulas radials, which are orientated with the smaller north-south current. For the same reasons a  $u$  and  $v$  component comparison in Liverpool Bay is expected to find a high  $u$  and low  $v$  correlation as was found by Kelly<sup>15</sup> when comparing the dominant along-shelf and lesser cross-shelf current components (Table 1).

Howarth<sup>2</sup> compared the ADCP and HF WERA radar current time series for Liverpool Bay using data collected in 2006. The complex correlations between the HF radar and ADCP were determined to be 0.94 and 0.93 at A and B, respectively and the  $M_2$  tidal amplitudes and phases were found to have high agreement. The rms difference between radar and ADCP calculated in other studies ranges from 5–20 cm/s<sup>-1</sup> and higher correlations are generally associated with smaller rms differences, as found by Teague,<sup>14</sup> but this is not always the case, as shown by Fernandez and Paduan.<sup>12</sup> Generally rms differences for good correlations, as expected in Liverpool Bay, will be around 8–12 cm/s<sup>-1</sup> (Table 1). The rms difference will also be related to the magnitude of the current being considered, as larger currents have the potential for larger differences in magnitude, as found by Fernandez and Paduan,<sup>12</sup> when low amplitudes resulted in an rms difference of 8.5 cm/s<sup>-1</sup>, but the time series only had a correlation of 0.4.

The ADCP configuration in Liverpool Bay has a theoretical accuracy for determining currents of 0.7 cm/s<sup>-1</sup>. Due to the sampling frequency the theoretical accuracy of each radial measured by the Liverpool Bay WERA radar is 9 cm/s<sup>-1</sup>, significantly larger than the ADCP. This, however, is improved by finding the peak of a quadratic fitted to the logged values of the Doppler spectra around the Bragg-scattering first order peak. When the two radials are combined for a dual current vector their cross-over angle,  $\beta$ , and the current alignment relative to the radial,  $\alpha$ , introduces an error magnification that will be less than 1.5 for  $\beta < 1.3\alpha$  and less than 4 when  $\beta > 30^\circ$ .<sup>4</sup> The angle between two radials is generally required to be  $>30^\circ$  and  $<150^\circ$  when resolving for the current vector.<sup>29</sup>

The amplification factor is greatest where the difference in look angle approaches  $180^\circ$ , however, in Liverpool Bay this region is also outside the required  $60^\circ$  region from the bore-sight of the radar, where side lobe contamination is prevalent and dual currents and waves are not resolved. Chapman and Graber<sup>19</sup> showed these geometric errors can be estimated by using the HF radar radial current measurements and the component of the ADCP current in the direction of the radial being considered.<sup>4</sup> This eliminates cross-over as it is a single radar measurement. An estimate for the magnitude of the cross-over angle error can be obtained by taking the difference between the rms difference of the ADCP and radar radial current and the rms difference between the ADCP and the dual current vector.

Howarth<sup>2</sup> used an ADCP bin at a constant height above the bed to compare directly with the HF radar surface current, 18.5 m at site A and 20.5 m at site B. Site A has the largest water depth variation and the 18.5 m bin varies between 2 and 10 m below the surface in a mean water depth of 24 m. In order to be directly compared with results from<sup>2</sup> the same bins have been used for this HF radar-ADCP comparison. A pressure

sensor mounted on the ADCPs gives the height of the water column at that location and is used to select the correct bin height above the bed to produce a 2 m and 3 m below-surface time series. This is also compared to the various radar current measurements as well as the ADCP measurements for a constant bin height to see if a particular method gives significantly different results.

The comparison is based on hourly values of HF radar and ADCP measurements available between 1 January 2006 and 31 December 2007. Outliers occur in both current time series but are more prevalent in the HF radar measurements. Physically unrealistic current speeds for Liverpool Bay were removed from both the HF radar and ADCP time series before comparison applying a threshold of 4 times the average current speed. The threshold value was required to filter out spikes of obvious instrument error in the data and not intended to filter measurement noise or mask real measurement differences between the ADCP and HF radar. The current time series from both the ADCP and HF radar were inspected and this threshold was found to include over 99% of the time series data in all datasets with only very large spikes being removed.

## TIDAL ANALYSIS

The method of Least Squares harmonic analysis tidal decomposition was applied to both the radar and various depth ADCP  $u$  and  $v$  currents following the method in Emery and Thomson.<sup>30</sup> This method is commonly used for tidal analysis<sup>13, 15, 31, 32</sup> as it easily incorporates large gaps and missing data points. This method also has the advantages of being able to pick out the amplitudes and phases of specific frequencies which is especially useful due to the known celestial forcing of the tides,<sup>33</sup> and is less intensive computationally than, for example, a Fast Fourier Transform (FFT). The FFT also requires a continuous time series requiring interpolation of the data for the many small gaps of an hour or less as well as gaps of up to a few days reducing the validity of the results.<sup>30</sup>

Howarth<sup>2</sup> reported 90% of the observed current variance in Liverpool Bay to be due to tidal forcing with the semi-diurnal tides dominant, and also compared the semi-diurnal  $M_2$  tidal constituent ellipse parameters as quality indicators of the HF radar measurement and found close agreement with ADCP A and B.

Amplitudes and phases for 10 tidal frequencies were obtained from the ADCP and HF radar current time series. These frequencies cover a range of the main tidal forcing frequencies significant in Liverpool Bay and are the diurnal  $O_1$  and  $K_1$ , semi-diurnal,  $N_2$ ,  $M_2$ ,  $S_2$ , and  $K_2$ , and a sample of their subsequent harmonics,  $MS_4$ ,  $S_4$ ,  $M_4$ , and  $M_6$ . Calculations using an extended selection of 20 tidal frequencies were also considered but not found to improve results. The amplitude and phase of each tidal frequency can be used to construct an estimated current time series which can then be subtracted from the original data to obtain the residual time series.

The tidal residual time series can also be used to investigate wind forcing on surface currents and show how surface effects vary at different depths of ADCP measurement. Ebuchi<sup>32</sup> defined the residual time series as the HF radar current minus the ADCP current. This assumes the ADCP bin

and the surface currents are the same and removes more of the tidal energy compared to subtracting the calculated tide from the observation, which maintains some tidal energy most likely cause by a slightly varying phase. With this Ebuchi found weak positive correlation between both components of the current vectors of 0.26 and 0.4 and linear regressions slopes between residual current and wind velocity to be of the order of typical magnitudes for wind drift.

In this study both definitions of residual current are applied and the resulting residual time series are compared with the wind velocity measurements taken on Hilbre Island (Fig 1).

RADIAL RESULTS

Radial currents from several radar cells were compared with ADCP currents in the radar measurement direction 18m above the bed at ADCP A (ADCP-A<sub>ab18</sub>) and at 20m above the bed at ADCP B (ADCP-B<sub>ab20</sub>), a selection of which are given in Table 2. All correlations were calculated at the 95% significant level, or greater, and found to have a confidence interval of  $\pm 0.01$  or better.

Formby radial measurements have correlations of  $0.96 \pm 0.002$  at the 99% confidence limit with both ADCP A<sub>ab18</sub> and B<sub>ab20</sub>. The Llanddulas current radial correlations with ADCP

Mooring and Measurement details		r		RMSD cm/s		Mean current speed cm/s			
						Radar		ADCP	
ADCP A <sub>ab18</sub> – R234	Radial – Llanddulas	0.87		10		17		17	
ADCP B <sub>ab20</sub> – R136	Radial – Llanddulas	0.82		11		15		16	
ADCP A <sub>ab18</sub> – R234	Radial – Formby	0.96		13		37		37	
ADCP B <sub>ab20</sub> – R136	Radial – Formby	0.96		13.8		39		36	
ADCP A <sub>ab18</sub> – R198 (wf)	Radial – Formby	0.87		17.2		29		29	
ADCP A <sub>ab18</sub> – R217 (wf)	Radial – Formby	0.89		16.3		29		30	
ADCP B <sub>ab20</sub> – R198 (wf)	Radial – Formby	0.91		14.1		29		29	
ADCP B <sub>ab20</sub> – R217 (wf)	Radial – Formby	0.93		16.8		37		39	
		u	v	u	v	u		v	
						Radar	ADCP	Radar	ADCP
ADCP A <sub>ab18</sub> – R234	Component form East (u) and North (v) ADCP and dual radar currents	0.97	0.58	13.3	11.8	37.7	37.6	11.2	8.1
ADCP A <sub>bs2</sub> – R234		0.95	0.70	14.5	9.7		36.9		9
ADCP A <sub>bs3</sub> – R234		0.96	0.61	12.6	10.6		38.7		8.7
ADCP B <sub>ab20</sub> – R136		0.98	0.57	14.3	10.4	41.6	39.5	10.3	11
ADCP B <sub>bs2</sub> – R136		0.94	0.72	16.9	7.3		38.2		11.7
ADCP B <sub>bs3</sub> – R136		0.97	0.71	12.3	8.4		40.2		11.5
ADCP A <sub>bs2</sub> – ADCP A <sub>bs3</sub>		0.99	0.96	8	3				
ADCP B <sub>bs2</sub> – ADCP B <sub>bs3</sub>		0.97	0.87	12	6				
ADCP A <sub>ab18</sub> – R198 (wf)		0.82	0.28	30.3	26.8	42.5		15.9	
ADCP A <sub>ab18</sub> – R217 (wf)		0.83	0.27	30	29	42.9		18.9	
ADCP B <sub>ab20</sub> – R198 (wf)		0.88	0.40	26.2	26.5				
ADCP B <sub>ab20</sub> – R217 (wf)		0.89	0.40	25.7	29.1				
							Radar		ADCP
ADCP A <sub>ab18</sub> – R234	ADCP and dual Radar complex current measurement (phase degrees)	0.93 (2.4)		14.3				39	
ADCP A <sub>ab3</sub> – R234		0.83 (9.67)		21		41.0		28.4	
ADCP A <sub>bs2</sub> – R234		0.93 (0.05)		13.9				39.1	
ADCP A <sub>bs3</sub> – R234		0.93 (–0.05)		13.7				40.6	
ADCP B <sub>ab20</sub> – R136		0.94 (–2.7)		14.6				42	
ADCP B <sub>ab3</sub> – R136		0.89 (2.43)		22		44.1		30	
ADCP B <sub>bs2</sub> – R136		0.92(–0.06)		15.8				41.2	
ADCP B <sub>bs3</sub> – R136		0.95 (0.07)		12.3				42.9	
		u	v	u	v	u		v	
						Radar	ADCP	Radar	ADCP
ADCP A <sub>ab18</sub> – R234	Residual current of ADCP and dual radar in East (u) and North (v) component form	0.38	0.18	12.4	12.2	9.1	8.3	8.5	5.6
ADCP A <sub>bs2</sub> – R234		0.42	0.45	10.2	10		9.7		6.8
ADCP A <sub>bs3</sub> – R234		0.48	0.42	12.2	11.8		8.6		6.1
ADCP B <sub>ab20</sub> – R136		0.61	0.40	13.0	10.3	9.9	9.5	7.3	6.4
ADCP B <sub>bs2</sub> – R136		0.39	0.47	12.3	7.6		11.5		7.3
ADCP A <sub>bs3</sub> – R136		0.53	0.47	12.1	9.1		8.9		6.3

Table 2: Correlations, r, and root mean square differences, RMSD, between the 2006–2007 Liverpool Bay current time series from a 13 MHz HF-radar and 600 KHz ADCP. ADCPs are bed mounted and measurement bins are 2m and 3m below the surface (bs2 and bs3 respectively) or h metres above the bed (abh). Radar cell 234 (R234) is co-located with ADCP A and radar cell 136 (R136) is co-located with ADCP B. Wind farm (wf) cells are R198 and R217. Mean current speeds in cm/s, where the absolute value of the current velocity is averaged, is also listed

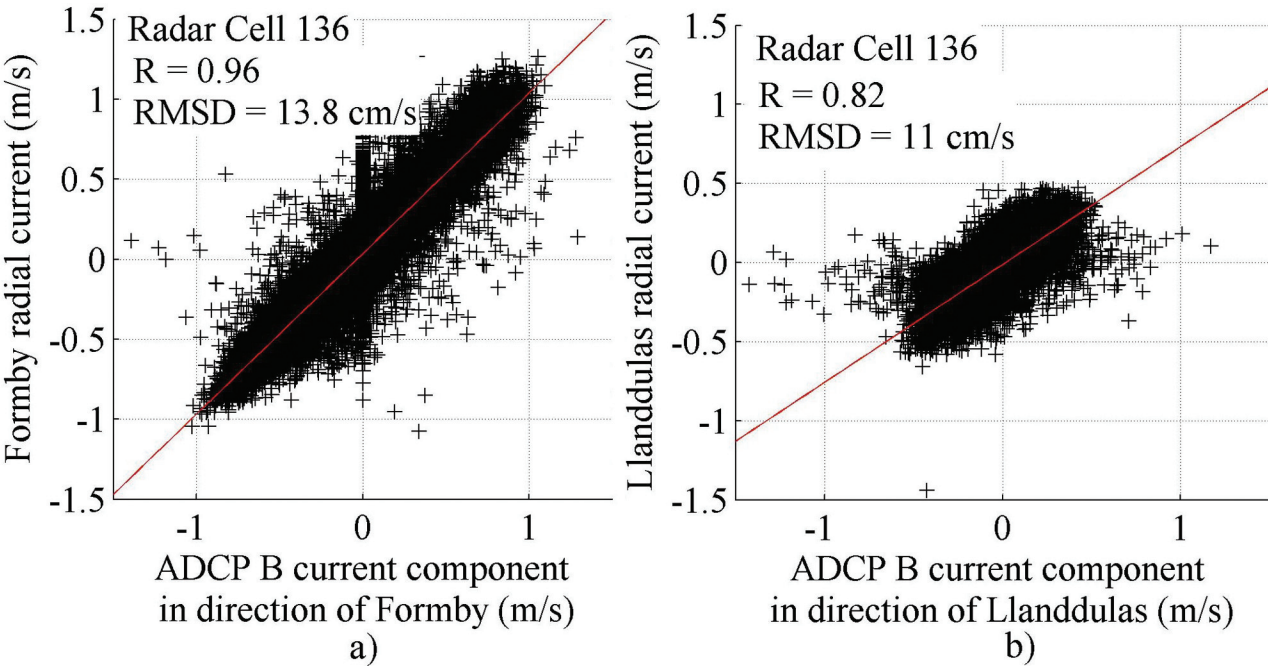


Fig 2: The comparison of HF radar cell 136 radial currents from a) Formby and b) Llanddulas with the ADCP B component of current in the measurement direction for a two-year time series. R is the correlation and RMSD the root mean square difference

A,  $0.87 \pm 0.004$ , and ADCP B,  $0.82 \pm 0.005$ , at the 99% confidence limit are lower than for Formby but the results still exceed those found in previous investigations (see Table 1). Previous HF radar and ADCP correlations, including Fernandez and Paduan,<sup>12</sup> using a 25MHz OSCAR radar, and those of Emery<sup>16</sup> and Paduan,<sup>28</sup> both of whom used a 13MHz CODAR radar, had correlations ranging between 0.5 and 0.72. Previous studies have, however, used ADCP data from 9m and 20m below the ocean surface which is below the measurement averaging depth of the HF radars.

Fig 2 shows HF radar cell 136 radial currents from a) Formby and b) Llanddulas compared with ADCP-B<sub>ab20</sub>. The component of the current in the direction of Llanddulas is clearly seen to be smaller in magnitude than that of Formby, with an average current magnitude of almost half (see Table 2). This causes a larger rms differences between the Formby HF radar and the ADCPs,  $13 \text{ cm/s}^{-1}$  and  $13.8 \text{ cm/s}^{-1}$  with ADCPs A<sub>ab18</sub> and B<sub>ab20</sub>, respectively, compared with those between the Llanddulas HF radar and the ADCPs,  $10 \text{ cm/s}^{-1}$  and  $11 \text{ cm/s}^{-1}$  at ADCP A<sub>ab18</sub> and B<sub>ab20</sub> respectively. These rms differences also fall mid-range of those previously reported, but are smaller compared with their mean current magnitude.

Table 2 also gives the correlations for ADCPs A and B with the Formby HF radar radials at cells 198 and 217, which are co-located with the North Hoyle wind farm. ADCP B is in closer proximity to the wind farm and has better agreement than ADCP A for these cells with higher correlations of 0.91 and 0.93 and smaller rms differences of  $14.1 \text{ cm/s}^{-1}$  and  $16.8 \text{ cm/s}^{-1}$  at cells 198 and 217, respectively. The correlations at the wind farm are less than at the ADCP locations but they are still in excellent agreement and exceed those of previous studies; however the rms differences are notably

larger. Other influencing factors such as measurement angle and distance from the ADCP are likely to have the biggest impact on current agreement in this region.

U AND V RESULTS

The comparison of the u and v current components between radar cell 136 and ADCP-B<sub>ab20</sub> are shown in Figs 3a and b respectively. Fig 3 reflects Fig 2 and clearly demonstrates the domination of the east-west currents in Liverpool Bay with the north-south component having a mean magnitude of roughly 25% that of the east-west current (see Table 2). The correlations of the u component between the radar and ADCPs are much higher than found in previous studies, being  $0.97 \pm 0.001$  with the ADCP-A<sub>ab18</sub> and  $0.98 \pm 0.001$  with ADCP-B<sub>ab20</sub>, both at the 99% confidence limit. The correlations for the north current component are  $0.58 \pm 0.01$  and  $0.57 \pm 0.01$ , again at the 99% confidence limit, for ADCP-A<sub>ab18</sub> and ADCP-B<sub>ab20</sub> respectively. These are significantly less than for the u component but compare well with the correlation of 0.58 for the non-dominant current component between the radar-ADCP study by Paduan and Rosenfeld.<sup>34</sup>

The rms differences are reasonable compared to radar-ADCP comparisons overall but are towards the large end of the rms difference range of  $6.2\text{--}13.3 \text{ cm/s}^{-1}$  found in previous studies for component currents,<sup>12, 14, 34</sup> (see Table 1). Despite the large correlation differences in Liverpool Bay between u and v components the rms differences are similar. Therefore the rms difference expressed as a percentage of the mean current magnitude is thought to better indicate the level of agreement between the radar and ADCP measurements, as was the case for radial currents.



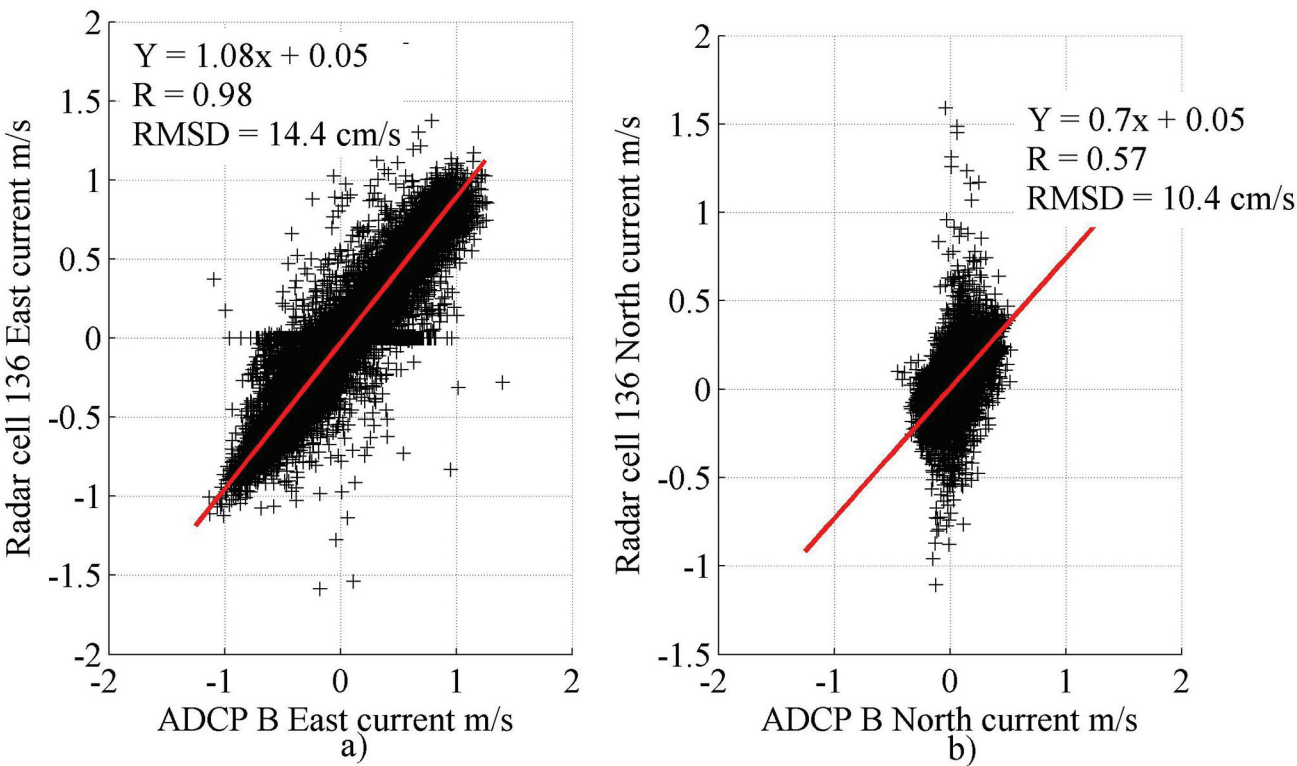


Fig 3: The comparison of the East and North components of radar cell 136 and ADCP B for a two-year current time series. R is the correlation and RMSD the root mean square difference

ADCP measurements at 2m and 3m below the surface were also compared as u and v components with the radar (Table 2). For ADCP currents 2m below the surface the rms difference was found to be larger than those at a constant bin height by an average of  $2\text{cm/s}^{-1}$ , however using ADCP currents at 3m below the surface improved the rms difference by an average  $1\text{cm/s}^{-1}$ . This may indicate that the ADCP current is noisier at 2m below the surface possibly due to side lobe contamination from the surface. This is supported by the fact that at ADCP B the rms difference at 2m below the surface was  $4\text{cm/s}^{-1}$  larger than at 3m for the u component.

The vector currents in component form were considered for the wind farm location (Table 2). The correlations at the wind farm are consistent with their distance from the ADCP but this is not the case for the rms difference. Fig 4 shows that the rms difference for the u (a) and v (b) components increases with distance from the ADCP but at cells 198 and 217 it is over double the average for that same distance. Other outliers are also present on Fig 4, however these are not co-located with the wind farm. As such the wind farm is not thought to be the main cause of the outliers. Another contributing factor to differences at the wind farm location is the cross-over angle,  $\beta$ .

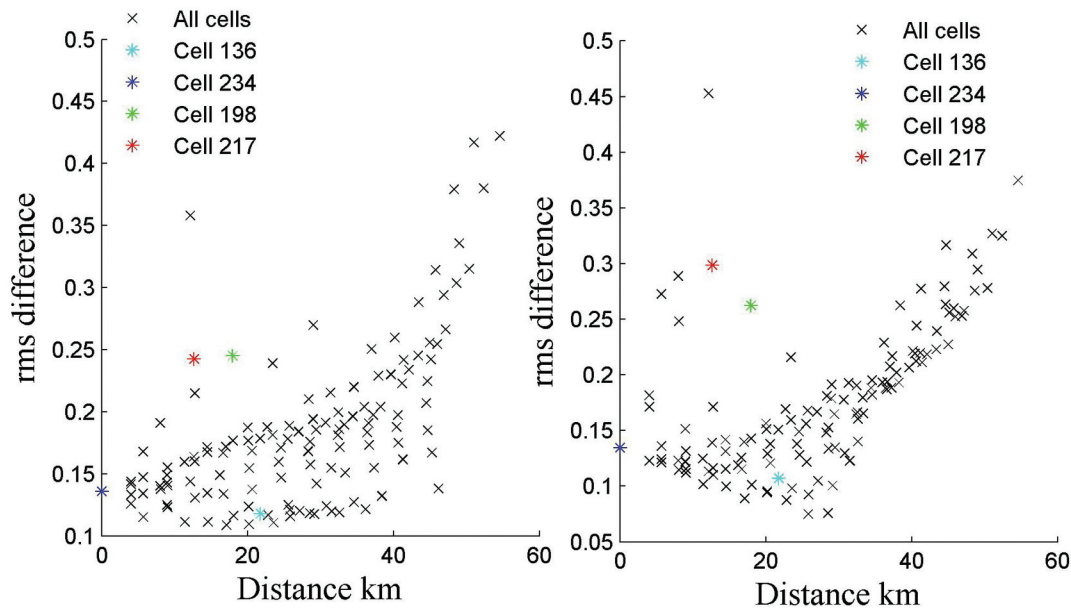


Fig 4: The root mean square, rms, difference (m/s) between the east, a), and north, b), dual radar current component and ADCP A current 18m above the bed against distance from the ADCP

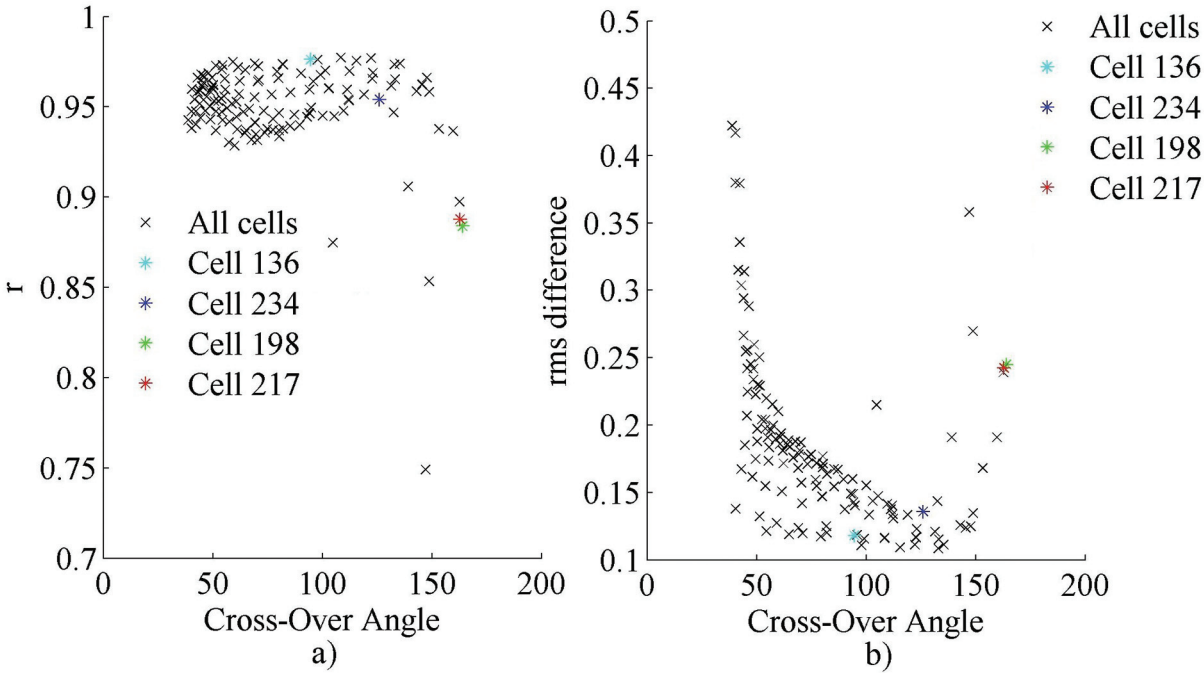


Fig 5: a) The correlation,  $r$ , between the dual radar east current and ADCP B current 20m above the bed against cross-over angle. b) The root mean square, rms, difference (m/s) between the dual radar east current component and ADCP B current 20m above the bed against cross-over angle

Fig 5a demonstrates how the correlation between the radar and ADCP varies with cross-over angle. For the majority of cells this is excellent compared with previous studies and most outliers occur for angles greater than  $150^\circ$  as expected.<sup>29</sup> Fig 5b shows how the rms difference between the radar and ADCP varies with the cross-over angle and is a distinctive ‘U’ shape. Cells 198 and 217 have large rms differences but these appear consistent for the cross-over angle at these locations,  $164^\circ$  and  $163^\circ$  for cells 198 and 217 respectively. The radar dual current vectors and radial current difference have been used to estimate the magnitude of the crossover angle error as set out by Chapman and Graber.<sup>19</sup> The cross-over angle at the NHWF is therefore estimated to introduce errors in the current amplitudes of roughly  $15\text{cm/s}^{-1}$ . For cells within the recommended range this is much less, roughly  $3\text{cm/s}^{-1}$ .

COMPLEX CORRELATION RESULTS

Treating the  $u$  and  $v$  currents as real and imaginary components of a complex number the Pearson product-moment correlation coefficient between the radar and ADCPs were calculated using a circular correlation function. Current vectors from radar cell 234 and ADCP- $A_{ab18}$  have a correlation of magnitude 0.93 and argument  $2.4^\circ$  (Table 2). These results are very similar compared to the complex correlation of magnitude 0.94 and argument  $1.5^\circ$  found by Howarth<sup>2</sup> when comparing the same measurement system for a one-year time series in 2006, as was the case for radar cell 136 and the ADCP- $B_{ab20}$ . At both locations the ADCP and radar correlation is high and the currents agree to within a similar order of the azimuthal resolution of the radar. The rms differences are again towards the larger end of the range compared to

previous studies but are acceptable as they are a smaller percentage of the mean current magnitude.

Howarth<sup>2</sup> found the complex correlation magnitude between the radar and ADCPs to be less for the bin 3m above the bed than at the 18m and 20m bins and this was also the case for the two-year extended time series. The mean currents magnitudes at the bed were found to be approximately 25% less, possibly due to shearing forces, current stratification and bed friction. The complex correlation magnitudes between the bed and the surface calculated<sup>2</sup> for ADCP- $A_{ab3}$  of 0.93 and 0.92 for ADCP- $B_{ab3}$  compare well to the values found for the two-year current comparison of 0.83 and 0.89 for ADCP- $A_{ab3}$  and  $B_{ab3}$  respectively (Table 2). The directional agreement is also reasonable, within  $10^\circ$  of each other, given the different ADCP deployments and is again close to the directional resolution of the radar. The high agreement between the ADCP bed level currents and the radar is another indication of how dominant the tidal forcing is within this region.

Comparing the radar and ADCP A currents 2 and 3m below surface (2m below the surface is regarded as the ADCP surface current) show exactly the same high correlations (Table 2) as for the constant ADCP- $A_{ab18}$  bin currents and rms differences within  $0.6\text{cm/s}^{-1}$  of each other. The ADCP A 3m below surface currents show a slight improvement in rms difference that those at 2m but it is small and overall the currents appear will mixed at this location, as was the case when comparing  $u$  and  $v$  components at 2m and 3m below the surface. This is also seen at ADCP B but in this instance the better agreement between the radar and ADCP currents at 3m below the surface is more significant. There is a noticeable decrease in the rms difference using ADCP currents at 3m below the surface at ADCP B and better agreement of the radar and ADCP mean magnitude and direction for both ADCP A and B.

TIDAL ANALYSIS RESULTS

Tidal analysis has been carried out on the vector current components. The ADCP and radar measured u components and the reconstructed tidal series are very well correlated, above 0.96, and have small rms differences of below 2cm/s<sup>-1</sup>. The weaker north components are still quite strongly correlated with the tidal reconstructed series, 0.68 or greater, and again have small rms differences. The radar and ADCP ellipses phases show good agreement within 3° and amplitudes with a difference of 2cm/s<sup>-1</sup>. This level of agreement was also seen by Prandle<sup>31</sup> who found the semi-major axis of the M<sub>2</sub> tidal frequency to have a precision of less than 0.5cm/s<sup>-1</sup> for a region where tidal currents are dominant.

The 10 tidal frequencies used are shown to account for most of the tidal variance. Table 3 shows the percentage of tidal energy removed by each of the 10 tidal constituents and their totals. The dominant tidal frequency is clearly seen to be the M<sub>2</sub> constituent accounting for over 77% of the u component amplitude and the 10 tidal frequencies together accounting for over 91%. The v component is seen to be less tidally dominated with the M<sub>2</sub> component accounting for between 22% and 40% and between 29% and 49% of the v current component is attributed to these 10 tidal frequencies in total.

Due to the lower percentage tidal frequency accounting for the v component amplitudes an extended set of 20 frequencies was tested, however these were not found to increase the percentage of energy removed by more than 1%.

Both the ADCP and radar appear to measure the tidal current amplitudes and directions with excellent agreement. How well they are capturing surface effects was investigated by looking at the correlations and rms differences between their residual currents (Table 2). The residual current is representative of forcing from tidal frequencies not used in the harmonic analysis, the wind driven current element, other surface process, and non-linear interactions. Most significant was the improvement in correlation of the radar and ADCP residual north component by taking the 2m or 3m below surface currents as opposed to the current at the constant bin height suggesting more surface effects are captured.

The correlations of the residuals with wind measurements taken on Hilbre Island (Table 4) were investigated to assess how this surface effect is measured by both the ADCP and HF radar. When including all available wind data correlations with the radar residual currents being moderate (around 0.4) agreement with ADCP is limited. Stronger winds are expected to have more of a forcing effect on the current and be indica-

Tidal Frequency	Percentage of tidal energy removed by specific tidal frequencies (%)							
	Radar 234 E	Radar 234 N	ADCP A <sub>ab18</sub> E	ADCP A <sub>ab18</sub> N	Radar 136 E	Radar 136 N	ADCP A <sub>ab20</sub> E	ADCP A <sub>ab20</sub> N
O <sub>1</sub>	0.020	0.10	0.03	0.048	0.023	0.029	0.019	0.028
K <sub>1</sub>	0.017	0.092	0.02	0.073	0.029	0.031	0.032	0.14
N <sub>2</sub>	2.24	1.06	2.63	0.86	1.73	1.41	1.83	0.84
M <sub>2</sub>	77.72	22.51	78.89	33.86	79.25	29.89	77.36	40.99
S <sub>2</sub>	9.34	3.25	10.1	5.46	9.48	6.08	10.68	6.34
K <sub>2</sub>	2.23	1.14	2.1	1.09	1.49	1.53	1.69	1.06
M <sub>4</sub>	0.23	0.66	0.22	1.44	0.29	0.44	0.15	0.12
MS <sub>4</sub>	0.038	0.21	0.043	0.33	0.036	0.017	0.0066	0.015
S <sub>4</sub>	0.0026	0.0007	0.0017	0.023	0.0022	0.0011	0.0012	0.020
M <sub>6</sub>	0.042	0.0097	0.018	0.048	0.021	0.067	0.053	0.16
Total	91.9	29.0	94.1	43.2	92.4	39.5	91.8	49.7

Table 3:The percentage of current attributed to the ten tidal frequencies used in the tidal analysis of data and in creating the residual current time series

Residual current time series	All wind speeds, 0 m/s + (Calm Winds +)		Wind speed >= 12 m/s (Strong Breeze +)	
	East	North	East	North
Radar Cell 136	0.38	0.44	0.47	0.77
Radar Cell 234	0.36	0.42	0.48	0.72
ADCP A <sub>bs2</sub>	0.07	0.33	0.01	0.30
ADCP A <sub>bs3</sub>	-0.02	0.26	-0.037	0.25
ADCP A <sub>ab18</sub>	-0.04	0.25	-0.06	0.26
ADCP B <sub>bs2</sub>	0.16	0.15	0.19	0.19
ADCP B <sub>bs3</sub>	0.12	0.094	0.09	0.079
ADCP B <sub>ab20</sub>	0.15	0.15	0.10	0.18
Radar 234 minus ADCP A <sub>ab18</sub>	0.39	0.29	0.47	0.57
Radar 136 minus ADCP B <sub>ab20</sub>	0.22	0.22	0.32	0.48

Table 4:Wind and residual current time series correlations. ADCPs are bed mounted and measurement bins are 2m and 3m below the surface (bs2 and bs3 respectively) or h metres above the bed (abh)

tive of higher sea state conditions and so a high-pass threshold was applied for winds  $>12.3\text{ms}^{-1}$  (12% of data), categorised as a strong breeze. The east component again showed moderate positive correlation, however the radar component  $v$  residuals at cell 234 and 136 were found to have much stronger correlations of  $0.72 \pm 0.02$  and  $0.77 \pm 0.02$  at the 95% confidence limit, respectively. This shows, particularly for the north direction, that wind driven current elements will account for a significant proportion of the residual current.

Correlations between wind and ADCP residuals are negligible at the 95% confidence limit for the ADCP measurements at a constant bin height and improve slightly when using the 2m and 3m below surface currents. Wind effects are therefore not propagating deep enough for the ADCP closest surface bin to be distinguishable above noise level and the radar, which directly observes the ocean surface, is best suited to observe surface wind effects.

Correlations with wind data using the alternative method for calculating residual surface current, as defined by Ebuchi<sup>32</sup> are also given in Table 4. It was found that for a strong breeze both the east and north currents had moderate correlations comparable to those found by Ebuchi, however these are not as good as when using the residual surface current calculated from tidal analysis.

## CONCLUSIONS

The continuous two-year time period has enabled data compared to have sampled a wide variety of environmental conditions. Currents in Liverpool Bay are found to be consistent over this period and the correlations between the ADCP and radar are greater than previously reported,  $>0.9$ . North-south currents in Liverpool Bay are on average 65% smaller than east-west currents which are tidally dominated by the  $M_2$  tidal frequency. Due to tidal dominance of the east-west direction the radar and ADCP currents are highly correlated at both surface and bed level.

The results show excellent agreement with Howarth<sup>2</sup> at ADCP- $A_{ab18}$  and  $B_{ab20}$ . Agreement between currents 3m above the bed is slightly less but still has a large positive correlation,  $>0.83$ . The rms differences were very similar between both radar-ADCP comparisons for magnitude and direction and are comparable to the differences found by previous studies. Although the rms differences are at the large end of the range found previously the mean current magnitude is much larger than the rms difference.

The results show surface effects are better observed by the radar than the ADCP, even when comparing the near surface ADCP bin, although this does improve on the comparison with the ADCP at a constant bin height. This is due to the fact that the radar observes these effects directly and the closest an ADCP measurement can be made is 2m below the surface. The residual correlations with wind data support the radar as the preferred method to observe surface effects from wind and there was significant positive correlation between the radar residual current with winds of  $12.3\text{ms}^{-1}$  or more.

Using currents in component form showed a significant advantage in using an ADCP current time series at 2m or 3m below the surface, compared with a constant bin height, particularly for comparing north components. For east cur-

rents there appeared to be no advantage to using the ADCP currents at 2m below the surface as the rms differences are increased and in this case the evidence suggests using the 3m below surface current is a better option. This is also evident when treating currents in vector form and better highlights differences between using an ADCP current at a constant bin height compared with one at a constant depth.

The ADCP averages through the water column in 1m bins, the centre of which is a varying height above the bed depending on the deployment. This results in the 2m below surface current time series including backscatter in the averaging from between 1.5 and 2.5m below the surface and may introduce some side lobe contamination from reflections off the surface. The 3m below surface current time series does not have this issue as backscatter is from 2.5 and 3.5m below the surface. This is evident in the greater correlations and smaller rms differences found for the 3m below surface current compared to the 2m below surface current.

The wind farm region has consistently yielded lower correlations and larger rms differences between the radar and ADCP current measurement. After consideration this is thought to be a combination of degradation due to the large cross-over angle,  $\beta$ , and distance from the ADCPs location and not a direct consequence of the wind farm itself. Comparing the radial and dual current results the cross-over angle in the wind farm location is thought to introduce errors in the current amplitudes of roughly  $15\text{cm/s}^{-1}$ , and roughly  $3\text{cm/s}^{-1}$  in regions where the cross-over angle is within the required range. The wind farm is expected to have a greater influence on waves than on currents as the first-order linear ocean backscatter has a much better signal to noise ratio than the second-order side bands that characterise the non-linear response of the ocean surface used for wave measurements.

Overall the HF WERA radar in Liverpool Bay has been shown to provide consistent current measurements over a significant period of time with considerable accuracy over an extensive region, compared to current measurements made by ADCP. The radar is also shown to be a more appropriate tool to measure surface effects, compared to the bed mounted ADCP, in particular the observation of wind effects.

Future work in Liverpool Bay should include looking at a before and after comparison of the currents and waves at the Rhyl Flats wind farm by comparison with ADCP, buoy and POLCOMS model results, as the cross-over angle for this region is well within the accepted standard range.

## ACKNOWLEDGEMENTS

This work was supported by the Natural Environmental Research Council [grant number 14208] and the National Oceanography Centre.

## REFERENCES

1. Howarth MJ, Proctor R, Knight PJ and Smithson MJ. 2006. *The Liverpool Bay Coastal Observatory – towards the goals*. Proceedings of Oceans 2006, 18–21 September, Boston IEEE, pp6.



2. Howarth MJ, Player RJ, Wolf J and Siddons LA. 2007. *HF radar measurements in Liverpool Bay, Irish Sea*. Proceedings of Oceans 2007, 18–21 June, Aberdeen IEEE, pp6.
3. Howlett ER, Howarth MJ and Rippeth TP. 2008. 2008 *Liverpool Bay: a coastal sea's responses to winds, waves, tides and freshwater*. In: PECS 2008: Physics of Estuaries and Coastal Seas, Liverpool, UK, 25–29 August 2008. Liverpool, 29–31.
4. Prandle D. 1991. *A new view of near-shore dynamics based on observations from HF radar*. Progressive Oceanography 27, 403–438.
5. Wolf J, Osuna P, Howarth MJ and Souza AJ. 2007. *Modelling and measuring waves in coastal waters*. Proceedings of ICCE 2006, Vol. 1, 539–551, San Diego.
6. Crombie DD. 1955. *Doppler spectrum of sea echo at 13.56 Mc./s*. Nature, 175, 681–682.
7. Barrick DE. 1977. *Extraction of wave parameters from measured HF radar sea-echo Doppler spectra*. Radio Science, 12(3), 415–424.
8. Barrick DE, Evans MW and Weber BL. 1977. *Ocean surface currents mapped by radar*. Science, 198, 138–144.
9. Wyatt LR, Green JJ, Gurgel KW, Nieto Borge JC, Reichert K, Hessner K, Gunther H, Rosenthal W, Sætra O and Reistad M. 2003. *Validation and intercomparison of wave measurements and models during the EuroROSE experiment*. Coastal Engineering 48, 1–28.
10. Wyatt LR, Green JJ, Middleditch A, Moorhead MD, Howarth J, Holt M and Keogh S. 2006. *Operational wave, current and wind measurements with the Pisces HF radar*. IEEE Journal of Oceanic Engineering, 31, 819–834.
11. Terray EA, Brumley BH and Strong B. 1999. *Measuring waves and currents with an upward-looking ADCP*. Proceedings of the IEEE Sixth Working Conference on Current Measurement, 66–71. ISSN 0-7803-5505-9.
12. Fernandez DM and Paduan JD. 1996. *Simultaneous CODAR and OSCAR measurements of ocean surface currents in Monterey Bay*. Proceedings, IEEE IGARSS'96, Lincoln, NE, 3, 1749–1752.
13. Graber HC, Haus BK, Chapman RD and Shay LK. 1997. *HF radar comparisons with moored estimates of current speed and direction: Expected differences and implications*. Journal of Geophysical Research 102(C8), 18,749–766.
14. Teague CC, Vesecky JF and Hallock ZR. 2001. *A comparison of multifrequency HF radar and ADCP measurements of near-surface currents during COPE-3*. Journal of Oceanic Engineering 26(3), 399–405.
15. Kelly FJ, Bonner SJ, Perez JC, Trujillo D, Weisberg RH, Luther ME and He R. 2003. *A comparison of near-surface current measurements by ADCP and HF-radar on the West Florida Shelf*. IEEE/OES Proceedings of the Seventh Working Conference on Current Measurement Technology AP-25(1), 52–61.
16. Emery BM, Washburn L and Harlan JA. 2004. *Evaluating radial current measurements from CODAR high-frequency radars with moored current meters*. Journal of Atmospheric and Oceanic Technology 21(8), 1259–1271.
17. Stewart RH and Joy JW. 1974. *HF radio measurements of ocean surface currents*. Deep Sea Research 21, 1039–1049.
18. Kundu PK. 1975. *Notes and correspondence: Ekman Veering near the ocean bottom*. Journal of Physical Oceanography, 6, 238–242.
19. Chapman RD and Graber HC. 1997. *Validation of HF radar measurements*. Oceanography 10(2), 76–79.
20. Krogstad HE, Wolf J, Thompson SP and Wyatt LR. 1999. *Methods for intercomparison of wave measurements*. Coastal Engineering 37, 235–257.
21. Wyatt LR, Thompson SP and Burton RR. 1999. *Evaluation of high frequency radar wave measurement*. Coastal Engineering 37, 259–282.
22. Lane A, Knight PJ and Player RJ. 1999. *Current measurement technology for near-shore waters*. Coastal Engineering 37, 343–368.
23. Ott MW. 2002. *An improvement in the calculation of ADCP velocities*. Journal of Atmospheric and Oceanic Technology, 19, 1738–1741.
24. Shearman EDR and Moorhead MD. 1988. *Pisces: A coastal ground-wave radar for current, wind and wave mapping to 200km ranges*. IGARSS'88 proceedings.
25. Gurgel K-W and Antonischki G. 1997. *Remote sensing of surface currents and waves by the HF radar WERA*. IEE Proceedings, Electronic Engineering in Oceanography 439, 211–217.
26. Gurgel K-W, Antonischki G, Essen H-H and Schlick T. 1999b. *Wellen Radar (WERA): A new ground-wave HF radar for ocean remote sensing*. Coastal Engineering 37, 219–234.
27. Gurgel K-W, Essen H-H and Kingsley SP. 1999a. *High frequency radars: physical limitations and recent developments*. Coastal Engineering 37, 201–218.
28. Paduan JD, Kim KC, Cook MS and Chavez FP. 2006. *Calibration and validation of direction-finding high-frequency radar ocean surface current observations*. IEEE Journal of Oceanic Engineering 31(4), 862–875.
29. Paduan JD and Graber HC. 1997. *Introduction to high frequency radar: Reality and myth*. Oceanography 10(2), 36–39.
30. Emery WJ and Thomson RE. 2001. *Data analysis methods in physical oceanography*. Elsevier, Amsterdam, edition 2, 2001.
31. Prandle D. 1987. *The fine-structure of nearshore tidal and residual circulations revealed by HF radar surface current measurements*. American Meteorological Society 17(2), 231–245.
32. Ebuchi N, Fukamachi Y, Ohshima KI, Shirasawa K, Ishikawa M, Takatsuka T, Daibo T and Wakatsuchi M. 2006. *Observation of the soya warm current using HF ocean radar*. Journal of Oceanography, 62, 47–61.
33. Pugh DT. 1987. *Tides, surges and mean sea-level*. John Wiley & Sons, Chichester, edition 2.
34. Paduan JD and Rosenfeld LK. 1996. *Remotely sensed surface currents in Monterey Bay from shore based HF radar (Coastal Ocean Dynamics Application Radar)*. Journal of Geophysical Research, 101(C9), 20,669–20,686.
35. Kaplan DM, Largier J and Botsford LW. 2005. *HF radar observations of surface circulation off Bodega Bay (northern California, USA)*. Journal of Geophysical Research, 110, C10020.